

See discussions, stats, and author profiles for this publication at: <https://www.researchgate.net/publication/232927074>

# P-31-Edited Diffusion-Ordered H-1 NMR Spectroscopy for the Spectral Isolation and Identification of Organophosphorus Compounds Related to Chemical Weapons Agents and Their Degradat...

ARTICLE in ANALYTICAL CHEMISTRY · NOVEMBER 2012

Impact Factor: 5.64 · DOI: 10.1021/ac302788x · Source: PubMed

---

CITATION

1

---

READS

24

5 AUTHORS, INCLUDING:



Brian Mayer

Lawrence Livermore National Laboratory

21 PUBLICATIONS 102 CITATIONS

SEE PROFILE



Carlos A Valdez

Lawrence Livermore National Laboratory

26 PUBLICATIONS 249 CITATIONS

SEE PROFILE



Sarah C Chinn

Lawrence Livermore National Laboratory

49 PUBLICATIONS 399 CITATIONS

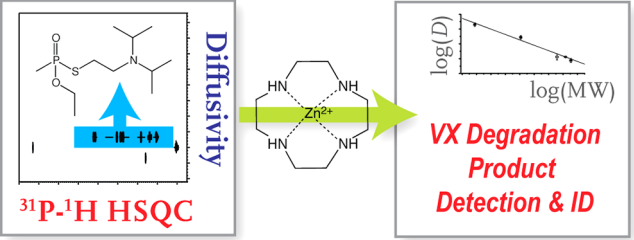
SEE PROFILE

# $^{31}\text{P}$ -Edited Diffusion-Ordered $^1\text{H}$ NMR Spectroscopy for the Spectral Isolation and Identification of Organophosphorus Compounds Related to Chemical Weapons Agents and Their Degradation Products

Brian P. Mayer,\* Carlos A. Valdez, Saphon Hok, Sarah C. Chinn, and Bradley R. Hart

Forensic Science Center, Lawrence Livermore National Laboratory, 7000 East Ave, Livermore, California 94550, United States

**ABSTRACT:** Organophosphorus compounds represent a large class of molecules that include pesticides, flame-retardants, biologically relevant molecules, and chemical weapons agents (CWAs). The detection and identification of organophosphorus molecules, particularly in the cases of pesticides and CWAs, are paramount to the verification of international treaties by various organizations. To that end, novel analytical methodologies that can provide additional support to traditional analyses are important for unambiguous identification of these compounds. We have developed an NMR method that selectively edits for organophosphorus compounds via  $^{31}\text{P}$ – $^1\text{H}$  heteronuclear single quantum correlation (HSQC) and provides an additional chromatographic-like separation based on self-diffusivities of the individual species via  $^1\text{H}$  diffusion-ordered spectroscopy (DOSY):  $^1\text{H}$ – $^{31}\text{P}$  HSQC-DOSY. The technique is first validated using the CWA VX (*O*-ethyl S-[2-(diisopropylamino)ethyl] methylphosphonothioate) by traditional two-dimensional DOSY spectra. We then extend this technique to a complex mixture of VX degradation products and identify all the main phosphorus-containing byproducts generated after exposure to a zinc-cyclen organometallic homogeneous catalyst.



Though emphasizing the criticality of the destruction of existing chemical-based weapons since the inception of the Chemical Weapons Convention (CWC) in 1997, the CWC's core mission has made the development of methodologies to assess, to surveil, and to analyze the presence of chemical weapons agents (CWAs) and their associated synthesis and degradation byproducts an equally important enterprise. A large majority of CWAs scheduled by the Organization for the Prohibition of Chemical Weapons (OPCW) are or are related to organophosphorus compounds with notable examples that include VX (*O*-ethyl S-[2-(diisopropylamino)ethyl] methylphosphonothioate), soman, and sarin. From a structural perspective, many CWAs are generally characterized by the presence of a phosphorus atom serving as an anchor point to which alkyl groups ( $\text{C}_1$ – $\text{C}_{10}$ ) may be bonded directly or indirectly (i.e., via the bridging intermediacy of a heteroatom such as O, S, or N).

Samples relating to OPCW inspections and proficiency examinations represent a wide variety of matrixes that may include aqueous or organic solutions, various soil types, or viscous/oily residues. Their analysis is typically characterized by sample preparatory methods that make the mixture amenable for chromatographic analyses combined with mass spectrometry (e.g., GC/MS and LC/MS). However, the correct identification of an analyte of interest can become a challenging task due to overwhelming interferences arising from the chemical compositions of the sample and the surrounding matrix. For this reason, the use of several methods in parallel

(so-called “hyphenated approaches”, e.g., LC-NMR) or multi-dimensional strategies (two-dimensional GC/MS) to attain a successful analysis is not only common but also often a necessary approach to take when dealing with these types of samples. For example, Hoggard and co-workers have employed 2D GC/MS combined with chemometric approaches to assess chemical impurity profiles and signatures associated with the nerve agent simulant dimethyl methylphosphonate.<sup>1</sup> The large number of impurities present in commercially manufactured material could only be fully characterized by employing a multidimensional chromatographic separation. As for hyphenated techniques, Mazumder and co-workers exploited high performance liquid chromatography coupled to solid-phase extraction and nuclear magnetic resonance (LC-SPE-NMR) for the analysis of the degradation of V-class agents and nitrogen mustard.<sup>2</sup> Only after LC separation were NMR spectra unambiguously attributable to single components, thereby making spectral identification of degradation signatures possible.

In the past twenty years, nuclear magnetic resonance (NMR) spectroscopy has gained considerable status as a powerful tool in the analysis and identification of toxic organophosphorus-based compounds. The high natural abundance and receptivity

**Received:** September 25, 2012

**Accepted:** November 5, 2012

**Published:** November 5, 2012

of both  $^1\text{H}$  and  $^{31}\text{P}$  nuclei make NMR an ideal tool for the analysis of phosphorus-containing CWAs. These natural properties in conjunction with advances in modern hardware technology, particularly in the field of cryoprobes, allow for the detection of relatively low concentrations ( $\sim 1$  ppm) of analytes within reasonable experimental time frames.

Samples originating from actual, real world scenarios often contain an unidentifiably large number of components that effectively prohibit the ultimate utility of  $^1\text{H}$  NMR, as signals related to phosphorus-containing CWAs will very likely be buried under or masked by those of solvents, dominant impurities, etc. Heteronuclear NMR ( $^{31}\text{P}$  or  $^{19}\text{F}$  in the cases of sarin and soman, for example) offers several solutions to this complex scenario in that (1) typically fewer resonances will be encountered, (2) heteronuclei generally enjoy wider native chemical shift ranges than that of  $^1\text{H}$  nuclei, and (3) splitting patterns due to J-coupling provide some limited insight into the structural details of the alkyl side chains. Despite these advantages, it is often undesirable to directly detect signals from phosphorus and fluorine, as they are not as sensitive as proton nuclei in an absolute sense. Therefore, proton-heteronucleus correlation experiments that detect on the proton channel but contain information about couplings to other nuclei have become critical in CWA analysis by NMR. In particular, one- and two-dimensional  $^1\text{H}$ – $^{31}\text{P}$  heteronuclear single quantum coherence (1D/2D  $^1\text{H}$ – $^{31}\text{P}$  HSQC) is a highly effective experiment that spectrally edits out proton signals not directly involved in phosphorus-containing compounds due to lack of  $^1\text{H}$ – $^{31}\text{P}$  J-coupling. This approach in combination with total correlation spectroscopy sequences (e.g., HSQC-TOCSY) often allows for unequivocal structural elucidation of alkyl and heteroalkyl side chains.<sup>3–5</sup>

The majority of HSQC-based NMR techniques employed for studying phosphorus-containing CWAs have been two-dimensional correlation methods. That is, the information contained in both dimensions is *spectral* in nature, where, for example, cross peaks indicate J-coupled protons and phosphorus nuclei. Considering the relatively narrow proton chemical shift range, mixtures containing even low numbers of phosphorus-containing compounds can render HSQC-edited proton spectra difficult to interpret, particularly for one-dimensional data. For this reason, an alternative approach for the analysis of complex proton spectra has centered around the concept of diffusion-ordered spectroscopy (DOSY).<sup>6,7</sup> In this technique, the detected proton signals are separated on the basis of the self-diffusion coefficients of individual molecules. DOSY then amounts essentially to a chromatographic-type separation, where diffusivity appears along the traditional  $F_1$  (or indirect) dimension of the 2D spectrum as opposed to chemical shift. In combination with the HSQC methods described above, one can in principle edit out all proton signals but those J-coupled to phosphorus nuclei and establish a direct relationship between the remaining resonances and their respective diffusivities.

Several authors have reported on the design and practical application of HSQC-DOSY and related techniques in the past, but this work has only focused on carbon ( $^{13}\text{C}$ ) as the heteronucleus in question.<sup>8–10</sup> For example, McLachlan and co-workers<sup>10</sup> detail a constant time gradient 3D HSQC-DOSY variant to distinguish between chemical cognates, rutin and quercetin, that exhibit resonances with very similar chemical shifts in both the carbon and proton dimensions. Various groups have also used  $^{31}\text{P}$  DOSY in the past for various

applications.<sup>11–14</sup> Notably, Segev and co-workers effectively exploited phosphorus NMR diffusion measurements to characterize the binding of organophosphorus compounds (some being nerve agent simulants) to chymotrypsin.<sup>12</sup> The combination of  $^1\text{H}$  DOSY and  $^{31}\text{P}$  NMR heteronuclear correlation editing (via HSQC, for example) has not been addressed, however. In this work, we demonstrate  $^1\text{H}$ – $^{31}\text{P}$  HSQC-edited  $^1\text{H}$  DOSY for identifying phosphorus-containing CWAs from complex, proton-rich NMR spectra. Diffusion constants obtained via this route will be validated against traditional  $^1\text{H}$  DOSY spectra that have not been edited via HSQC. We will also consider the degradation products of VX, using the HSQC-DOSY sequence to not only isolate molecules containing organophosphorus groups but also identify unknown degradation products.

## SAMPLE PREPARATION

VX (O-ethyl S-[2-(diisopropylamino)ethyl] methylphosphonothioate, see inset Figure 2) was synthesized at LLNL (see safety note) and was purified via vacuum distillation ( $\sim 97\%$  purity by  $^{31}\text{P}$ ,  $^1\text{H}$  NMR, and GC/MS). Deuterated chloroform ( $\text{CDCl}_3$ , 99.96 atom % D, 0.03 (v/v) TMS) and deuterium oxide ( $\text{D}_2\text{O}$ , 99.9 atom % D) were purchased from Sigma-Aldrich (St Louis, MO.) and used as received for the preparation of the NMR samples. The preparation of the VX sample was done in enough volume of  $\text{CDCl}_3$  (typically between 400 and 550  $\mu\text{L}$ ) to yield a final concentration of roughly 1000 ppm VX. Because of the low volatility of VX and its associated degradation products, the tubes were simply capped, tightly sealed with ParaFilm, and kept under refrigeration. After execution of the experiment(s), the samples were immediately destroyed using a 10% bleach solution.

We also carried out a VX degradation experiment involving a base-induced process. This base-induced degradation of VX was carried out by dissolving VX (neat oil, 1.1 mg, 4.1  $\mu\text{mol}$ ) in  $\text{D}_2\text{O}$  (300  $\mu\text{L}$ ) in a 5 mm NMR tube followed by the sequential addition of a 0.39 mM  $\text{D}_2\text{O}$  solution of hexamethylphosphoramide (HMPA internal standard) (100  $\mu\text{L}$ , 0.7  $\mu\text{L}$ , 4.0  $\mu\text{mol}$ ) and a 20 mM  $\text{D}_2\text{O}$  solution of  $\text{Zn}^{2+}$ -cyclen catalyst (30  $\mu\text{L}$ , 0.6  $\mu\text{mol}$ ,  $\sim 15$  mol % to VX). The NMR tube was capped, sealed, and gently vortexed to ensure proper mixing of the components. HMPA was chosen as an internal standard for its excellent water solubility, its well-defined  $^{31}\text{P}$  and  $^1\text{H}$  NMR resonances (29.8 and 2.56 ppm, respectively), and its stability to both the catalyst concentration and the solution pH. The catalyst used in these experiments was  $\text{Zn}^{2+}$ -cyclen as its perchlorate salt and was prepared as described previously<sup>15</sup> and was chosen for its ability to generate reactive hydroxyl ion species that are able to degrade organophosphorus compounds.

**Safety Note.** VX is a highly toxic compound that can harm exposed individuals at extremely small doses (e.g., dermal  $\text{LD}_{50} < 0.1$  mg/kg<sup>16</sup>). Only properly trained personnel, in a certified laboratory possessing the adequate equipment to carry out their synthesis and subsequent purification, should handle highly toxic chemical warfare agents. The Forensic Science Center at Lawrence Livermore National Laboratory (LLNL) has the authority and capability to synthesize and handle small quantities of VX through its accreditation as a United States Designated Laboratory for the Organization for the Prohibition of Chemical Weapons, which performs monitoring for verification of international treaties that ban chemical weapons.<sup>17</sup> Proper protective personal equipment (PPE) should be worn at all times which include lab coats, safety

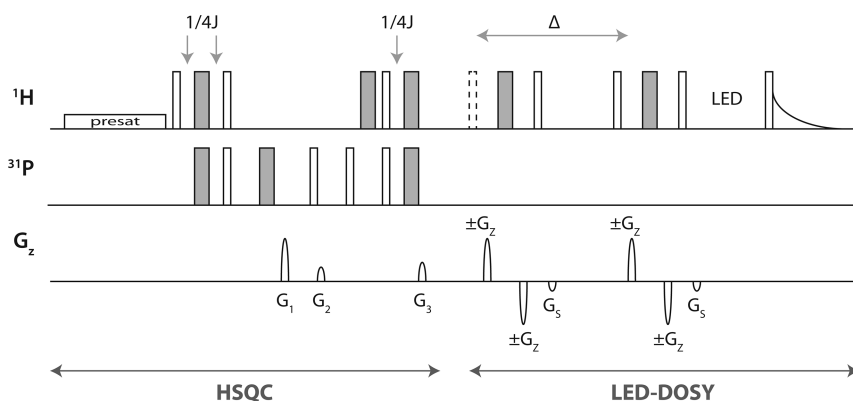


**Figure 1.**  $^1\text{H}$ – $^{31}\text{P}$  HSQC-DOSY experiment with solvent presaturation. Thin white rectangles and thick gray rectangles correspond to  $90^\circ$  and  $180^\circ$  pulses, respectively. During the excitation/reconversion segments of the double INEPT HSQC portion,  $J_{\text{HP}} = 15.8$  Hz was used to calculate the interpulse delay. The dashed  $90^\circ$  pulse traditionally used to initiate the DOSY experiment is omitted due to the presence of the preceding pulses (and therefore ignored from the phase table below).  $\Delta$  corresponds to the time between the center of the two positive gradient pulses,  $+G_z$ , and  $\delta$  is twice the duration of one positive gradient pulse,  $+2G_z$ . Gradient pulses are given in the bottom row:  $G_1 = 80\%$ ,  $G_2 = 30\%$ ,  $G_3 = 32.4\%$ ,  $G_5 = -13.17\%$ , and  $G_z$  was stepped from 2% to 95% of the maximum gradient strength of  $5.3 \text{ G cm}^{-1} \text{ A}^{-1}$ . The phase cycling is here given beginning with all proton pulses in order of left-to-right (dashed pulse omitted) and then following with the phases of the phosphorus and receiver channels.  $^1\text{H}$ :  $\{x\}_{\text{presat}}$ ,  $\{x\}$ ,  $\{x\}$ ,  $\{y\}$ ,  $\{x x - x - x\}$ ,  $\{y\}$ ,  $\{x\}$ ,  $\{x\}$ ,  $\{x x - x - x\}$ ,  $\{x x x x - x - x - x - x\}$ ,  $\{x\}$ ,  $\{x - x x - x - x x - x x\}$ ,  $\{x x x x - x - x - x - x\}$ ;  $^{31}\text{P}$ :  $\{x\}$ ,  $\{y y y y - y - y - y - y\}$ ,  $\{x\}$ ,  $\{-y\}$ ,  $\{x\}$ ,  $\{x - x\}$ ,  $\{x\}$ ; acquisition:  $\{x x - x - x x x - x - x\}$ .

glasses, butyl-based gloves with nitrile gloves underneath to provide further protection, and a face shield. The handling and preparation of the NMR samples should be conducted inside a well-ventilated and certified chemical fume hood.

## NMR EXPERIMENTAL SECTION

All experiments were executed on a Bruker Avance III 600 MHz instrument equipped with a Bruker TCI 5 mm cryoprobe (Bruker Biospin, Billerica, MA) at  $30.0 \pm 0.1$  °C. The basic pulse sequences used were canned experiments provided by the manufacturer (see below).

In addition to its low volatility and its similarity to a wide range of other organophosphorous compounds (e.g., pesticides), VX was chosen due to its favorable NMR line shape characteristics. Many phosphates, phosphonates, and other phosphorus-containing molecules containing alkoxy side groups off the central phosphorus nucleus (e.g., sarin, soman) are  $\text{HH}'\text{P}$  systems from an NMR perspective. The remote  $\text{H}'$  proton affects the HSQC signal, generating distorted, weak peaks despite  $^4J_{\text{H}'\text{P}} \approx 0$  due to antiphase terms that evolve during the INEPT transfer periods.<sup>5</sup> As also discussed, a Q3 Gaussian cascade pulse was shown to be an effective  $180^\circ$   $^1\text{H}$  refocusing pulse, as  $J_{\text{HP}}$  heteronuclear scalar coupling does not evolve during the application of the pulse. More importantly, the homonuclear coupling is refocused by this selective  $180^\circ$  pulse, and antiphase terms otherwise modulating the detectable magnetization are removed.

In the case of VX, the methyl group directly bound to the phosphorus nucleus dominates the evolution of the detectable magnetization, and little antiphase character is observed in the line shape. Therefore, the present experiments require no band-selectivity, as the direct phosphorus-methyl bond yields a strong, in-phase HSQC peak (ca. 1.82 ppm, isolated HP system) when the experiment is optimized for the  $^2J_{\text{HP}} \approx 15.6$  Hz coupling (delay is  $1/(2J_{\text{HP}})$ ). Conventional 1D  $^1\text{H}$ – $^{31}\text{P}$  HSQC spectra were obtained using the *hsqcgpnd1d* sequence provided by the hardware manufacturer. The proton and phosphorus carrier frequencies were 4.53 and 30.00 ppm, respectively; and the proton spectral window was 10.08 ppm.

The nominal  $^1\text{H}$  and  $^{31}\text{P}$  excitation pulse widths were 15.25 and 9.00  $\mu\text{s}$ , respectively; and the recycle delay was set at 5 s. This delay was determined to be sufficient for proton relaxation ( $T_1$ s on the order of 1 s), and though  $^{31}\text{P}$  nuclei may not relax completely, quantitation (through  $^1\text{H}$  peak intensities) is not a primary focus for this current work.

For the conventional DOSY experiment (Bruker sequence *ledbpgp2s*), 32 gradient strengths were selected between 2% and 95% of the maximum pulsed gradient strength of  $5.3 \text{ G cm}^{-1} \text{ A}^{-1}$ . Sixteen scans were taken per gradient strength for a total experimental time of approximately 45 min. The data were processed using the commercial software provided by the manufacturer. Considering the nature of the sample and the relatively well-resolved spectra, single component data fitting was determined to be satisfactory (vis-à-vis more complicated inverse Laplace algorithms).

Two versions of the HSQC-DOSY pulse sequence were created for the present work. The first resulted from simply appending on the *ledbpgp2s* sequence to the end of the *hsqcgpnd1d* experiment with minor modifications to the phase cycling of the pulses. The second sequence was identical to the first except for a low power presaturation pulse (1 s, 0.154 mW) prior to the first excitation pulse on the  $^1\text{H}$  channel. This experiment is shown schematically along with phase cycling in Figure 1. It is important to point out the nontraditional receiver phasing in these experiments. In order suppress the effects of undesirable terms in the detectable magnetization (in a product operator sense), the receiver phases of the nominal HSQC and DOSY pulse sequences were added together in a cyclical fashion.

## RESULTS AND DISCUSSION

**Distilled VX.** Figure 2a shows the one-dimensional proton spectrum of the synthesized VX sample. VX peaks and additional peaks related to the NMR solvent are both identified on the spectrum. Because the synthesis results were purified by distillation, it is not surprising to have a relatively clean, well-resolved NMR spectrum. This observation will be exploited when testing the HSQC-DOSY experiment against results



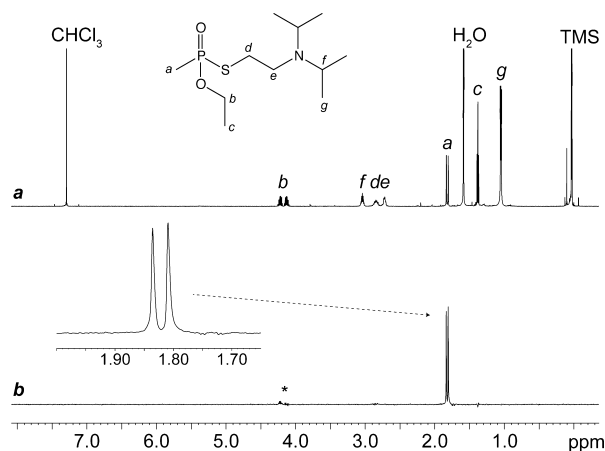


**Figure 2.** (a)  $^1\text{H}$  spectrum of the distilled VX sample. Solvent impurities identified, and the structure of VX and resonance assignments given. (b) 1D  $^1\text{H}$ - $^{31}\text{P}$  HSQC ( $J = 15$  Hz) spectrum showing  $\text{CH}_3$ -P doublet. An inset shows the doublet in more detail. The asterisk represents some small antiphase signal from the ethoxy methylene protons.

obtained by the more routine, manufacturer supplied DOSY sequence.

Figure 2b shows the 1D  $^1\text{H}$ - $^{31}\text{P}$  HSQC spectrum of the same sample showing the  $\text{CH}_3$ -P doublet associated with VX. It contains only the signal arising from the protons on the methyl group directly bound to the phosphorus atom (with a small artifact from methylene protons on the ethoxy group). For complex  $^1\text{H}$  spectra, this type of spectral editing is important for two reasons: (1) only  $^1\text{H}$  signals originating from protons coupled to phosphorus appear, making spectra considerably less cluttered, and (2) the receiver gain of the spectrometer hardware can be set higher, so that those signals are much more intense on a signal per scan basis. This enhanced sensitivity allows for significantly shorter experimental times relative to a straight  $^1\text{H}$  or  $^{31}\text{P}\{^1\text{H}\}$  experiment, and coupled with diffusion-ordered spectroscopic strategies, HSQC offers a powerful tool comparable to few other NMR techniques for sensitive detection of analytes of interest at low concentrations.

To assess the accuracy of the HSQC-DOSY technique, we first turn attention to traditional diffusion-ordered experiments. Figure 3 shows the results of the DOSY experiment using the *ledbpgp2s* sequence. Note that the raw NMR data has been phased and baseline corrected before execution of the DOSY analysis. A brief look at the figure reveals that seven proton signals share a common diffusivity and can therefore be assigned to the protons of VX (with confirmation 1D/2D NMR and library spectra). At the current experimental conditions ( $30^\circ\text{C}$  in  $\text{CDCl}_3$ ), the diffusivity of VX is  $D_{\text{VX}} = 1.37 \pm 0.04 \times 10^{-9} \text{ m}^2/\text{s}$ . Note that the line width of the fully processed DOSY spectrum reflects the uncertainty in the derived diffusivity. The three remaining peaks belong to tetramethylsilane,  $\text{CHCl}_3$ , and residual water, and their diffusivities are  $3.23 \pm 0.05 \times 10^{-9} \text{ m}^2/\text{s}$ ,  $3.27 \pm 0.12 \times 10^{-9} \text{ m}^2/\text{s}$ , and  $6.93 \pm 0.10 \times 10^{-9} \text{ m}^2/\text{s}$ , respectively. These results were then used to validate the HSQC-DOSY sequence.

Figure 4 shows the results for the  $^{31}\text{P}$ -edited HSQC-DOSY experiment for the identical distilled VX sample used above. Shown is the normalized peak intensity for the methyl doublet as a function of gradient strength. Because VX is the sole

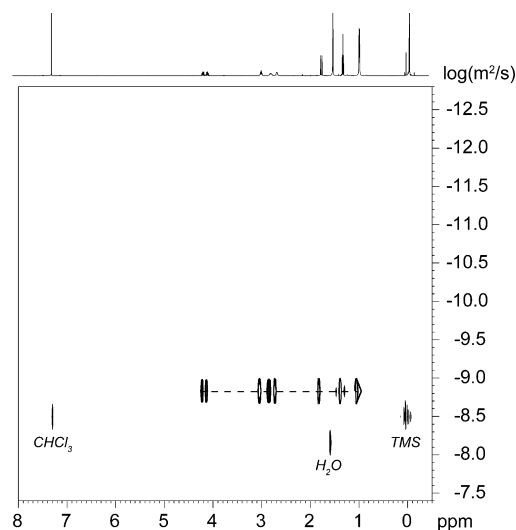


**Figure 3.** Traditional 2D DOSY plot using *ledbpgp2s* sequence showing  $\log(D)$  on the y-axis. The solvent peaks have been identified explicitly, and the VX peaks have been highlighted with a dashed line. From this plot,  $D_{\text{VX}}$  was determined to be  $1.37 \pm 0.04 \times 10^{-9} \text{ m}^2/\text{s}$ .

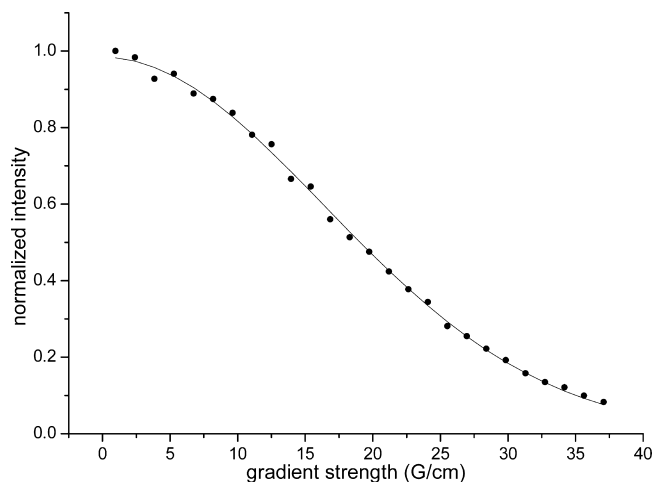


**Figure 4.** HSQC-DOSY decay for distilled VX solution (in  $\text{CDCl}_3$ ,  $30^\circ\text{C}$ ) as a function of gradient strength (filled circles). The curve is a nonlinear least-squares fit to the NMR data using eq 1.

phosphorus-containing molecule in the sample, we only observed a single peak in the HSQC-DOSY spectrum (recall Figure 2b). These data were fit to the traditional expression valid for bipolar, simulated echo-type DOSY experiment given as:

$$A(z, \Delta + \delta) = I_0 \exp[-D\gamma^2 g(z)^2 \delta^2 (\Delta - \delta/3)] \quad (1)$$

where  $I_0$  is the initial intensity (ca. unity),  $D$  is the diffusivity,  $\gamma$  is the proton gyromagnetic ratio,  $g(z)$  is the gradient strength (independent variable), and  $\Delta$  and  $\delta$  are the durations discussed in Figure 1. The data were fit using the commercially available software package Mathematica (Wolfram, IL, USA). The results from the distilled VX analysis using the HSQC-DOSY sequence gave  $D_{\text{VX}} = 1.32 \pm 0.05 \times 10^{-9} \text{ m}^2/\text{s}$ , which agrees quite well (within 5%) with the full, unedited DOSY sequence (vide supra). Now that the HSQC-DOSY sequence has been confirmed to give identical results to a traditional DOSY experiment, we now turn our focus to applying this

technique to a more complex system: VX degradation and resultant product identification.

**VX Degradation and Product Identification.** Assessing the efficacy of organic or inorganic small molecules toward degrading CWAs not only involves confirming the destruction of the target analyte but also entails the identification of the resultant degradation products. This is of particular importance for VX where, depending on the decontamination conditions, degradation products can be just as toxic in a physiological sense as the parent molecule itself. For example, under neutral to alkaline conditions (pH = 7–10), P–O bond cleavage can dominate producing ethanol and EA2192 (S-(2-diisopropyl-aminoethyl) methylphosphonothioate), a chemical of similar toxicity and anticholinesterase properties (intravenous LD<sub>50</sub> between 0.24 and 0.825 times that of VX depending on species).<sup>18</sup> Identifying, then, the products of CWA degradation becomes quite important because there exists a strong motivation to develop decontamination strategies that obviate the generation of such toxic byproducts.

Figure 5 shows the <sup>1</sup>H spectrum of the degraded VX sample. There are a significant number of additional peaks as compared

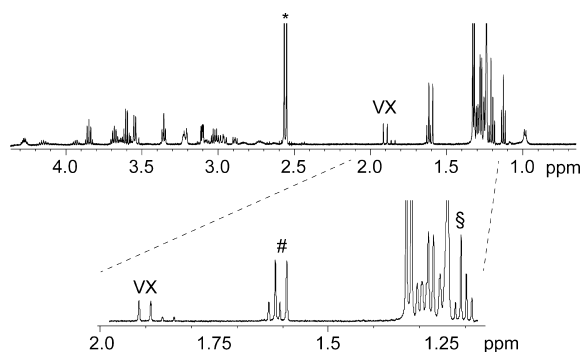


**Figure 5.** <sup>1</sup>H spectrum of the degraded VX sample (top). Note the complexity of the spectrum, particularly between 2.5 and 4.0 ppm and at approximately 1.25 ppm. The VX methyl doublet has been labeled, while an asterisk denotes the HMPA methyl doublet. The bottom spectrum highlights the 1.2–2.0 ppm region. Note the doublets marked as “VX” and “#”. A third, unresolvable signal (present, however, in the HSQC-DOSY spectrum, vide infra) is marked as “\$”.

to the distilled VX sample considered previously. The pattern of peaks suggests some VX-like byproducts, as the appearance of multiple doublets with J-couplings on the order of 10–15 Hz suggests several new CH<sub>3</sub>–P containing species. The goal of this work is to apply the HSQC-DOSY sequence to identify the primary degradation products. Note that, because we are only concerned with identifying the products associated with degradation, we did not let the reaction go to completion. Enough time passed simply to allow for measurable signals of degradation products to form (determined by monitoring NMR signals; ~4 h after introduction of the catalyst). For the DOSY analysis, we chose the four most intense resonances present: 2.610 ppm (HMPA), 1.901 ppm, 1.601 ppm, and 1.218 ppm. Though additional doublets were observed (e.g., one centered at 1.850 ppm), the poor signal-to-noise, given the experimental time, of the DOSY decay curves like that of Figure 4 prohibited confident extraction of diffusivities.

Because of the significant residual water signal in the NMR spectrum, the pulse sequence was prefaced with a low power presaturation pulse. The HSQC-DOSY experiment performed was identical to that of the distilled VX sample, and the data

obtained were similar in form to those in Figure 4. The decay curves were again analyzed using a nonlinear least-squares approach to yield the diffusivities of all major phosphorus-containing compounds. The decay data and goodness of fit for three of the four peaks (corresponding to HMPA, VX, and an unidentified compound) is given in Figure 6; note that the x-

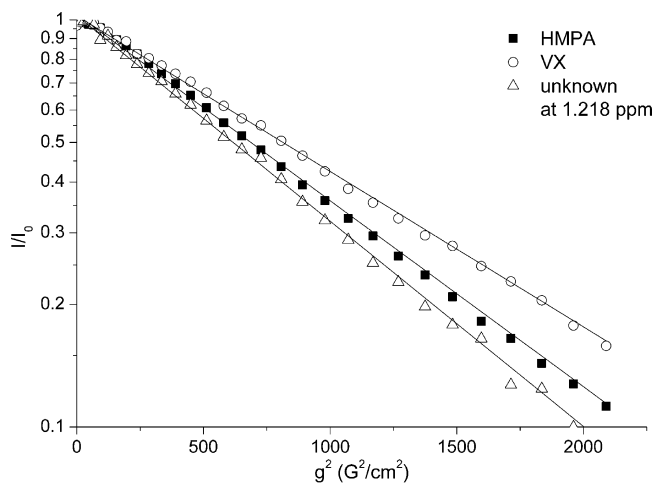


**Figure 6.** HSQC-DOSY decay curves for HMPA (filled squares), VX (open circles), and an unknown compound (open triangles). Note that these data are plotted differently than Figure 4; they have been “linearized” by plotting the intensity logarithmically against the square of the gradient strength.

axis is shown as the square of the gradient strength and the y-axis is logarithmic to show linearity of the data. The regression results are given in Table 1. Special note should be taken of the

**Table 1. Regression Results from HSQC-DOSY Data of the Degraded VX Solution<sup>a</sup>**

peak	chemical shift (ppm)	compound identity	$D$ ( $\times 10^{-10}$ m <sup>2</sup> /s)	$I_0$
2.610		HMPA	$7.45 \pm 0.09$	$1.03 \pm 0.01$
1.901		VX	$6.22 \pm 0.08$	$1.02 \pm 0.01$
1.601		— <sup>b</sup>	$6.39 \pm 0.12$	$1.02 \pm 0.01$
1.218		— <sup>b</sup>	$8.22 \pm 0.10$	$1.02 \pm 0.01$

<sup>a</sup>Four major phosphorus-containing compounds were easily measured. Given are the diffusivities and intensities for the various chemical shifts. HMPA and VX resonances have been identified. <sup>b</sup>Additional discussion of “unknown” compound identities in text.

two different measured diffusivities of VX. This results from the fact that two solvents of differing viscosities were used in the two examples presently given. For VX in CDCl<sub>3</sub> and D<sub>2</sub>O, the diffusivities are given by  $1.32 \times 10^{-9}$  and  $6.22 \times 10^{-10}$  m<sup>2</sup>/s, respectively.

We now turn to the identification of the two unidentified peaks at 1.601 and 1.218 ppm using the HSQC-DOSY data. Because we are using a cyclen-Zn<sup>2+</sup> catalyst for which the active degradation specie is a hydroxyl ion (HO<sup>−</sup>), the aqueous VX solution will be slightly basic. It has been established that between pH 7 and 10 there exists a competition between P–O and P–S bond cleavage of VX.<sup>18</sup> We would therefore expect that the primary resultant P-containing degradation products are ethyl methylphosphonic acid (EMPA, from P–S cleavage) and EA2192 (from P–O cleavage). Because of possible complexity of the <sup>1</sup>H spectrum, the low amounts of degradation

products produced, and the fact that we primarily only detect signals from  $\text{CH}_3\text{-P}$  doublets, distinguishing easily between these two products may prove difficult. HSQC-DOSY data, however, can yield considerable insight into the identification of the compounds at 1.601 and 1.218 ppm via their respective diffusivities.

The Stokes–Einstein relationship is often invoked to provide correlations between molecular size and weight to diffusivity. Under various assumptions, the smaller the molecule (i.e., the smaller its molecular weight), the faster it should diffuse in a given medium at constant viscosity and temperature. Upon consideration of the diffusivities in Table 1, one would conclude that the peak at 1.218 ppm with the largest diffusivity belongs to EMPA, as it is the suspected product with the lowest molecular weight. Library spectra and two-dimensional NMR techniques confirm this assignment. Because of the relatively low peak intensities at 1.601 ppm and the spectral complexity in this region, making a similar guess-and-check was not possible.

Direct relationships between molecular weight and DOSY-derived diffusivity have been exploited before to perform solution structure studies on unknown phosphorus-containing compounds.<sup>14</sup> In this work, a  $\text{MW} - D$  correlation was developed using a variety of trialkyl phosphates and used to determine the molecular weight of a phosphorus-containing organolithium compound. To derive an identity for the remaining peak at 1.601 ppm, we applied this technique using VX, HMPA, and EMPA as the calibrating species and determined an estimated molecular weight for the mystery compound.

Figure 7 plots the  $\log(D)/\log(\text{MW})$  correlation derived from the diffusivities of VX, EMPA, and HMPA. This curve was then

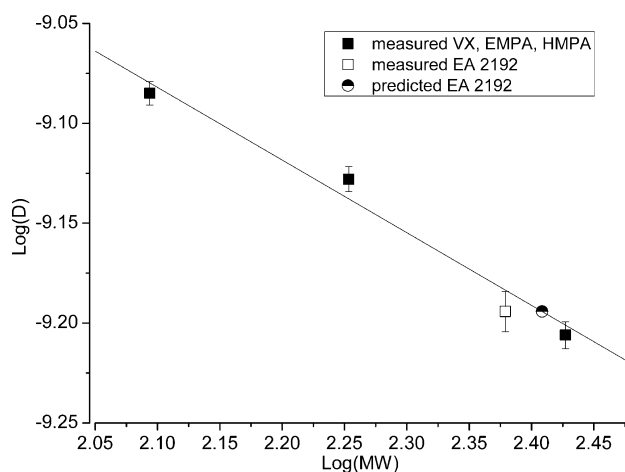


**Figure 7.**  $\log(D)/\log(\text{MW})$  correlation for VX, EMPA, and HMPA (filled squares). The line is a linear fit to those three points from which a predicted  $\log(\text{MW})$  for EA2192 is calculated (half-filled circle). The actual  $\text{MW}/\text{measured}$  diffusivity of EA2192 using the molecular weight of the compound is given by the open square.

used to predict the molecular weight of the compound at 1.601 ppm using its measured diffusivity of  $6.39 \times 10^{-10} \text{ m}^2/\text{s}$ . This calculation yields  $\log(\text{MW}) = 2.408$  or  $\text{MW} = 256 \text{ g/mol}$ . The fact that this compound's diffusivity is so close to that of the parent VX would lead to the conclusion that their molecular weights should be roughly similar. Considering the possible primary degradation chemistries resulting from exposure to the cyclen- $\text{Zn}^{2+}$  complex and the similarity in molecular weights,

we conclude that this compound is EA2192 with a molecular weight of 239.37. The calculated MW agrees well, ca. 7% of the actual molecular weight of EA2192. Comparison of chemical shifts of both the EA2192  $\text{CH}_3\text{-P}$  doublet and the  $^{31}\text{P}$  nucleus from previous research confirms the assignment of this toxic VX byproduct.<sup>19</sup>

## CONCLUSIONS

A strategy for the simplification of complex proton spectra using  $^{31}\text{P}$ -edited HSQC-DOSY sequences has been presented. These experiments were validated using traditional LED-DOSY techniques that lacked HSQC selectivity for samples related to chemical weapons and important not only for OPCW proficiency examinations and inspections but also for a wide variety of other organophosphorus containing compounds, particularly pesticides and other toxic environmental pollutants. We demonstrated that the HSQC-DOSY sequence could perform the efficient chromatographic-like separation necessary to isolate and identify the essential resonances related to VX degradation by a zinc-cyclen catalyst. Though the concentrations of the relevant compounds were kept to 100 to 1000 ppm for proof-of-concept purposes, more lengthy signal averaging in combination with modern cryoprobe technology will allow for detection of analytes at or possibly below 1 ppm. Self-diffusion of VX was also noted to slow when experiments were conducted in water, a more viscous solvent than chloroform; and we are currently assessing the ability of different solvent systems to provide higher "resolution" in the diffusion dimension (i.e., better chromatographic-like separation). Most importantly, however, the resultant HSQC-DOSY data were used to extract the identity of an "unknown" degradation product. Using a  $\log(D)/\log(\text{MW})$  correlation and an estimate for the unknown's molecular weight, we suspected this compound to be the well-documented degradation product EA2192 and were able to confirm this assignment based on literature references and other, more time intensive, multi-dimensional NMR techniques. This added benefit of the HSQC-DOSY sequence portends the application of this technique to assess the effects of various degradation agents (bleach, peroxides,<sup>20,21</sup> oximes, ozone,<sup>22</sup> etc.) and scenarios for which preferred degradation pathways and products are completely unknown.

## AUTHOR INFORMATION

### Corresponding Author

\*E-mail: mayer22@llnl.gov.

### Notes

The authors declare no competing financial interest.

## ACKNOWLEDGMENTS

This work was performed under the auspices of the U.S. Department of Energy by Lawrence Livermore National Laboratory under Contract DE-AC52-07NA27344.

## REFERENCES

- (1) Hoggard, J. C.; Wahl, J. H.; Synovec, R. E.; Mong, G. M.; Fraga, C. G. *Anal. Chem.* **2010**, 82 (2), 689–698.
- (2) Mazumder, A.; Kumar, A.; Purohit, A. K.; Dubey, D. K. *J. Chromatogr., A* **2010**, 1217 (17), 2887–2894.
- (3) Koskela, H.; Rapinaja, M. L.; Kuitunen, M. L.; Vanninen, P. *Anal. Chem.* **2007**, 79 (23), 9098–9106.
- (4) Koskela, H.; Ervasti, M.; Bjork, H.; Vanninen, P. *Anal. Chem.* **2009**, 81 (3), 1262–1269.

- (5) Koskela, H.; Hakala, U.; Vanninen, P. *Anal. Chem.* **2010**, *82* (12), 5331–5340.
- (6) Johnson, C. S., Jr. *Prog. Nucl. Magn. Reson. Spectrosc.* **1999**, *34* (3, 4), 203–256.
- (7) Kimmich, R., *NMR: tomography, diffusometry, relaxometry*; Springer: Berlin, 1997.
- (8) Gozansky, E. K.; Gorenstein, D. G. *J. Magn. Reson., Ser. B* **1996**, *111* (1), 94–96.
- (9) Barjat, H.; Morris, G. A.; Swanson, A. G. *J. Magn. Reson.* **1998**, *131* (1), 131–138.
- (10) McLachlan, A. S.; Richards, J. J.; Bilia, A. R.; Morris, G. A. *Magn. Reson. Chem.* **2009**, *47* (12), 1081–1085.
- (11) Kapur, G. S.; Cabrita, E. J.; Berger, S. *Tetrahedron Lett.* **2000**, *41* (37), 7181–7185.
- (12) Segev, O.; Columbus, I.; Ashani, Y.; Cohen, Y. *J. Org. Chem.* **2005**, *70* (1), 309–314.
- (13) Paulusse, J. M. J.; Huijbers, J. P. J.; Sijbesma, R. P. *Macromolecules* **2005**, *38* (15), 6290–6298.
- (14) Kagan, G.; Li, W.; Hopson, R.; Williard, P. G. *Org. Lett.* **2009**, *11* (21), 4818–4821.
- (15) Koziol, L.; Valdez, C. A.; Baker, S. E.; Lau, E. Y.; Floyd, W. C.; Wong, S. E.; Satcher, J. H.; Lightstone, F. C.; Aines, R. D. *Inorg. Chem.* **2012**, *51* (12), 6803–6812.
- (16) Council, N. R. *Review of acute human-toxicity estimates for selected chemical warfare agents*; National Academy Press: Washington, DC, 1997.
- (17) Love, A. H.; Vance, A. L.; Reynolds, J. G.; Davisson, M. L. *Chemosphere* **2004**, *57*, 1257–1264.
- (18) Munro, N. B.; Talmage, S. S.; Griffin, G. D.; Waters, L. C.; Watson, A. P.; King, J. F.; Hauschild, V. *Environ. Health Perspect.* **1999**, *107* (12), 933–974.
- (19) Brevett, C. A. S.; Sumpter, K. B.; Pence, J.; Nickol, R. G.; King, B. E.; Giannaras, C. V.; Durst, H. D. *J. Phys. Chem. C* **2009**, *113* (16), 6622–6633.
- (20) Smith, B. M. *Chem. Soc. Rev.* **2008**, *37* (3), 470–478.
- (21) Wagner, G. W.; Procell, L. R.; Sorrick, D. C.; Lawson, G. E.; Wells, C. M.; Reynolds, C. M.; Ringelberg, D. B.; Foley, K. L.; Lumetta, G. J.; Blanchard, D. L. *Ind. Eng. Chem. Res.* **2010**, *49* (7), 3099–3105.
- (22) Wagner, G. W.; Bartram, P. W.; Brickhouse, M. D.; Connell, T. R.; Creasy, W. R.; Henderson, V. D.; Hovanec, J. W.; Morrissey, K. M.; Stuff, J. R.; Williams, B. R. J. *Chem. Soc.-Perkin Trans. 2* **2000**, *6*, 1267–1272.